On-line Selection of Stable Visual Landmarks under Uncertainty*

Inhyuk Moon, Jun Miura, and Yoshiaki Shirai

Dept. Computer-Controlled Mechanical Systems, Osaka University
Suita, Osaka 565-0871, Japan

Abstract

This paper proposes a method to autonomously select stable visual landmarks from observed features by stereo vision and a given 2D obstacle map. The robot selects as stable landmarks vertical line segments which are distinct and on a vertical plane, because they are expected to be observed reliably from various viewpoints. Due to the vision and motion error of the robot, the observed feature positions include uncertainty. This uncertainty can be reduced by matching the detected vertical plane which includes the features to a known plane in the map. The position of a selected feature is modeled by a probabilistic distribution on the known plane. The selection and modeling process is performed on-line to adapt to an actual lighting and background condition which varies depending on viewpoints. When the robot moves, it uses several, less uncertain landmarks to estimate its motion. Experimental results in real scenes show the validity of the proposed method.

1 Introduction

It is a fundamental function for a mobile robot to estimate its current state such as postion and orientation. When a robot moves by dead reckoning, the positional uncertainty is increased by motion error. Thus, it is a general method to use landmarks for localization. To perform reliable navigation, artificial patterns are often used as landmarks[1]. However, it is a reluctant work for us to arrange artificial landmarks. Visual features such as vertical edges of door or obstacle are used as landmarks[2, 3]. However, such features may not be *stable*, that is, may not be observable under various conditions of lighting and background scene changed by viewpoints[4]. Therefore, it is desirable to determine stable landmarks based on observed data.

*Proc. of IROS-99, pp. 781-786, Kyongju, Korea, Oct. 1999.

Many researcher used learning and execution strategies with human assistance in order to select landmarks from observed data[5, 6]. The robot tries to construct a landmark map in the learning phase, and then it executes a given mission while estimating its own state based on the landmark map. But, these approaches need such a human assistance.

Horn and Schmidt[7] utilized vertical planar surfaces as landmarks. Sensed planar data by 3D laser range finder are matched to a given 3D map. However, the robot needed much computational efforts because the robot tried to detect planar information at each observation. In order to reduce the computational time, Talluri and Aggarwal[8], and Arsenio and Ribeiro[9] utilized boundary edges of obstacles instead of planar surfaces as landmarks. Visibility region map was constructed based on a given 3D map, and then the robot matches observed features to the map for localization. However, the boundary edges of obstacles may be unstable to the observation.

Since features which lie on a relatively planar surface are distinct over a wide range of viewpoints, Little et al.[10] utilized corner points on planar surfaces as stable landmarks using stereo data and corners. However, the study did not cosider uncertainty of vision, so matching results between frames should not be robust.

In this paper, we propose an on-line method of modeling and selecting visual landmarks under uncertainty of vision and motion, given a 2D obstacle map. Since a line is more stable feature than a point, the method selects *vertical line segments* on a planar surface as stable features. By matching a planar region including a subset of observed line segments to the corresponding *reference plane* on the given map, the positional uncertainty of the segments can be reduced. Then, the segment positions are modeled by a probabilistic distribution on the reference plane, and the segments are registered as landmarks. When the robot moves, it uses several, less uncertain landmarks to estimate its motion. Since the segment positions

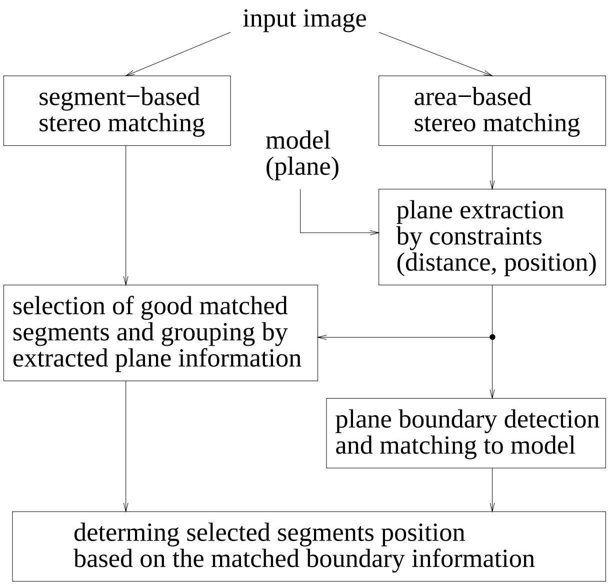

Figure 1: Processing flow of landmark selection.

are modeled by a probabilistic distribution, we set the state of the robot and landmarks to the system state to estimate repeatedly. When the robot observes a landmark, it can simultaneously estimate current own state and landmark state by Extended Kalman Filter.

Fig. 1 shows the processing flow for modeling and selecting stable visual landmarks. To extract stable vertical line segments, we use both segment- and area-based stereo matching methods. First, we match vertical line segments using the segment-based stereo mathing, and then false matched segments are filtered out by comparing with the *disparity image* obtained from the area-based stereo matching. Next, planar regions corresponding to given reference planes are extracted from the disparity image by using a positional constraint between the robot and the given plane, and then we group the filtered segments belonging to a planar region. Lastly, we search for a boundary position of the plane in the planar region. Then, relative positions of segments in the plane are estimated by matching the searched planar boundary to the given plane edge.

In the next section, we deal with a selection of stable features based on stereo observations, and then propose a method of modeling landmarks. Experimental results in real scenes show the validity of the proposed method. Lastly, we conclude the proposed methods in this paper.

2 Extracting stable vertical line features

2.1 Segment-based stereo matching

Vertical line segments are extracted from edges obtained by applying a horizontal differential operator to the input image. To match segments in the stereo images, we define similarity which consists of overlapping ratio, and orientation and length similarity, and then dynamic programming method is applied to determine the best matching by comparing the similarity[13].

In this paper, we represent the landmark state as 2D position on $X - Y$ workspace and the lowest and highest position on Z axis.

$$\boldsymbol{L} = [x \ y \ l_{low} \ l_{high}]^T \tag{1}$$

2.2 Area-based stereo matching

To extract planar surfaces, we use the area-based stereo matching method of which SAD is utilized as a criterion of matching. Since smaller value of SAD means more reliable matching, a false matching can be filtered out by setting a relevant threshold. The following equations express SAD between a pair of stereo images.

$$\begin{aligned} SAD_{RL} &= \sum_{(i,j)\in W} |I_R(i,j) - I_L(i+d,j)| \\ SAD_{LR} &= \sum_{(i,j)\in W} |I_L(i,j) - I_R(i-d,j)| \end{aligned} \tag{2}$$

where $I_L(i,j)$ and $I_R(i,j)$ denote intensities of pixel (i,j) in the stereo pair of images, and d denotes disparity. With two SAD results calculated from Eq. (2), we obtain a reliable matched disparity image by comparing disparity values between pixels in one disparity image and corresponding pixels in the other disparity image.

2.3 Planar surface extraction

Given a reference plane, we can predict a position where the plane is projected in the image, and the possible range of disparity of the plane. Then, we search for the pixels beloging to the predicted plane region in the disparity image. By applying a least sqaures method to the extracted disparity pixels, the plane is extracted.

2.3.1 Uncertainty of vertical line position on image

When a point on the 3D coordinates is projected into image, the projected position includes uncertainty due to a quantization error, which can be expressed by a random variable, and we model the error as Gaussian distribution with $\sigma_{img} = 0.5$[pixel].

Assuming that an observed vertical line segment is straight in the image and that each pixel to be composed of the line are independent, the horizontal positional uncertainty of the segment is inversely proportional to the number of pixels[11]. In this paper, we set the standard deviation of the position of line segment to σ_{img}.

2.3.2 Uncertainty of projection position in stereo images

When the robot with state $\boldsymbol{X}$ observes a vertical line $\boldsymbol{L}$ on the world coordinates, the projected position $\boldsymbol{I} = [x_l \ x_r]$ in stero images can be obtained by the stereo geometry[3], and it is expressed by a non-linear equation as follows:

$$\boldsymbol{I} = \boldsymbol{J}(\boldsymbol{X}, \boldsymbol{L}) \tag{3}$$

The covariance matrix of $\boldsymbol{I}$ is obtained by linearization as follows:

$$\boldsymbol{\Sigma}_I = \frac{\partial \boldsymbol{J}}{\partial \boldsymbol{X}} \boldsymbol{\Sigma}_X \frac{\partial \boldsymbol{J}}{\partial \boldsymbol{X}}^T + \frac{\partial \boldsymbol{J}}{\partial \boldsymbol{L}} \boldsymbol{\Sigma}_L \frac{\partial \boldsymbol{J}}{\partial \boldsymbol{L}}^T \tag{4}$$

If the line $\boldsymbol{L}$ has no uncertainty such as a known edge of reference plane, the positional uncertainty only depends on the robot uncertainty $\boldsymbol{\Sigma}_X$ as follows:

$$\boldsymbol{\Sigma}_I = \frac{\partial \boldsymbol{J}}{\partial \boldsymbol{X}} \boldsymbol{\Sigma}_X \frac{\partial \boldsymbol{J}}{\partial \boldsymbol{X}}^T \tag{5}$$

In this paper, as we define that 3σ is boundary of uncertainty, a valid region for searching is set to the following equation:

$$u - 3\sigma \leq valid\ search\ region \leq u + 3\sigma \tag{6}$$

where u denotes the mean value.

Then, the predicted position in images can be calculated by Eqs. (3)(4)(6).

2.3.3 Uncertainty of disparity

Disparity is expressed by subtraction of a pair of stereo projected positions x_l and x_r.

$$d = x_l - x_r + \nu \tag{7}$$

where ν denotes a pixel error with $E[\nu] = 0$ and ${\sigma_\nu}^2 = 2{\sigma_{img}}^2$. Since x_l and x_r can be obtained by stereo geometry when a 3D point $\boldsymbol{O} = [c_x \ c_y]$ in camera coordinates is given, we can rewrite Eq. (7) in the following equation[3]:

$$d = F\frac{c_x + B}{c_y} - F\frac{c_x - B}{c_y} + \nu = F\frac{2B}{c_y} + \nu \tag{8}$$

where F and $2B$ denote focal length and baseline, respectively. If we introduce the robot state $\boldsymbol{X}$ in order to transform camera coordinates to world coordinates, Eq. (8) can be expressed as the following non-linear equation:

$$d = D(\boldsymbol{X}) + \nu \tag{9}$$

As Eq. (9) is linearized by the Taylor series expansion around the mean $\hat{\boldsymbol{X}}$, the disparity uncertainty is obtained as follows:

$${\sigma_d}^2 = \frac{\partial D}{\partial \boldsymbol{X}} \boldsymbol{\Sigma}_X \frac{\partial D}{\partial \boldsymbol{X}}^T + {\sigma_\nu}^2 \tag{10}$$

2.3.4 Searching and fitting for planar region

Using the valid search region of Eq. (6) with the mean d of Eq. (9) and the standard deviation σ_d obtained from Eq. (10), we can pick up valid disparity pixels corresponding to a given reference plane in valid search position on the disparity image.

Since the reference plane is represented as a line on the 2D map, it is expressed by the following line model.

$$y = a + bx \tag{11}$$

where a and b are line parameters.

By applying a least squares method, we fit the disparity data to the plane model of Eq. (11). As a result, we obtain the line parameter and its covariace matrix.

2.4 Selecting line segments on planar region

Using the planar region obtained above, we choose a subset of segments from observed ones by investigating pixel being in the planar region corresponding to the position of pixels to be composed of each line segment. The selected segments belonging to the planar region regarded as stable features.

3 Modeling feature positions

Line segments belong to a planar region are modeled as landmarks. By matching the boundary postition of the planar region to the boundary edge of corresponding reference plane, we calculate the relative position of a selected segment with respect to the edge position. As the segment is constrained on the plane, its positional uncertainty can be reduced.

3.1 Combining two observations using Extended Kalman Filter

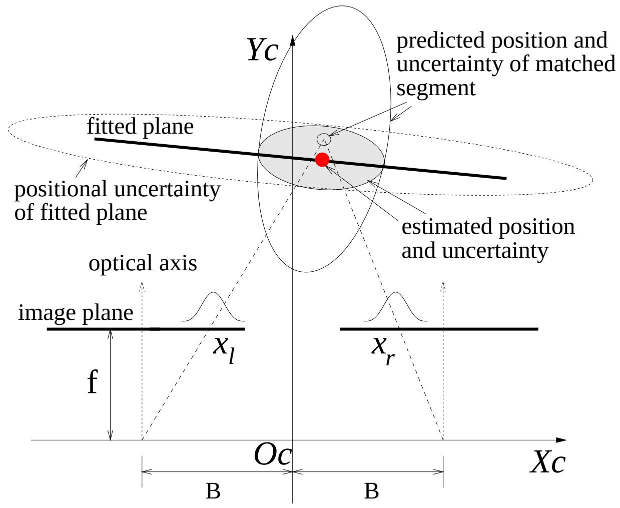

Figure 2: Combining two observation.

Two observations can be combined by using Kalman Filter (see Fig.2)[12]. The robot obtains two results which are a point obtained from segment-based stereo matching and a planar model estimated by fitting a set of disparity data. Since the point belongs to the reference plane, we can express the following constraint equation using Eq. (11).

$$c_y - (a + bc_x) = \boldsymbol{G}(\boldsymbol{L}_t, \boldsymbol{R}_t) = \mathbf{o} \tag{12}$$

where $\boldsymbol{L} = [c_x \ c_y]$ and $\boldsymbol{R} = [a \ b]$ denote a position and the line parameter corresponding to the reference plane, respectively. Linearizing Eq. (12) using Taylor series expansion, we express a new linear equation form as follows:

$$\boldsymbol{Y}_t = \boldsymbol{H}_t \boldsymbol{L}_t + \boldsymbol{V}_t \tag{13}$$

where

$$\boldsymbol{Y}_t = -\boldsymbol{G}(\tilde{\boldsymbol{L}}_t, \tilde{\boldsymbol{R}}_t) + \frac{\partial \boldsymbol{G}}{\partial \boldsymbol{L}_t} \tilde{\boldsymbol{L}}_t$$

$$\boldsymbol{H}_t = \frac{\partial \boldsymbol{G}}{\partial \boldsymbol{L}_t}$$

$$\boldsymbol{V}_t = \frac{\partial \boldsymbol{G}}{\partial \boldsymbol{R}_t}(\boldsymbol{R}_t - \tilde{\boldsymbol{R}}_t)$$

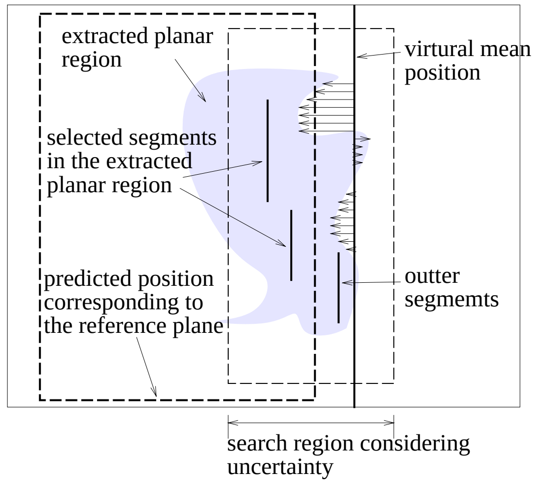

Figure 3: Searching for the boundary edge.

Based on the observation $\boldsymbol{Y}_t$ and its uncertainty $\boldsymbol{\Sigma}_{V_t}$, the position $\boldsymbol{L}_t$ corresponding to the point on the given plane can be estimated and updated using the Kalman Filter. $\boldsymbol{\Sigma}_{V_t}$ is expressed as follows:

$$\boldsymbol{\Sigma}_{V_t} = \frac{\partial \boldsymbol{G}}{\partial \boldsymbol{R}_t} \boldsymbol{\Sigma}_R \frac{\partial \boldsymbol{G}}{\partial \boldsymbol{R}_t}^T \tag{14}$$

where, $\boldsymbol{\Sigma}_R$ denotes covariance matrix of the fitted line obtained from section 2.3.4.

The Kalman Filter consists of the following equations:

$$\hat{\boldsymbol{L}}_t = \tilde{\boldsymbol{L}}_t + \boldsymbol{K}_t[\boldsymbol{Y}_t - \boldsymbol{H}_t \tilde{\boldsymbol{L}}_t]$$

$$\boldsymbol{\Sigma}_{\hat{L}_t} = [\boldsymbol{I} - \boldsymbol{K}_t \boldsymbol{H}_t] \boldsymbol{\Sigma}_{\tilde{L}_t}$$

$$\boldsymbol{K}_t = \boldsymbol{\Sigma}_{\tilde{L}_t} \boldsymbol{H}^T{}_t [\boldsymbol{H}_t \boldsymbol{\Sigma}_{\tilde{L}_t} \boldsymbol{H}^T{}_t + \boldsymbol{\Sigma}_{V\,t}]^{-1}$$

where $\hat{\boldsymbol{L}}_t$ and $\boldsymbol{\Sigma}_{\hat{L}_t}$ denote the estimated position and covariance matrix. $\tilde{\boldsymbol{L}}_t$ is the predicted position obtained by the stereo geometry, and $\boldsymbol{\Sigma}_{\tilde{L}_t}$ denote the predicted position and its covariance matrix. $\boldsymbol{K}_t$ is called the Kalman gain.

3.2 Searching for the boundary position

Assuming that the boundary edge is a vertical line, we first determine a search region in the extracted planar region obtained from section 2.3.2. Next, we set a horizontal position in the search region to a virtual mean (see Fig. 3). Then, we investigate differences between the mean position and boundary pixels in the planar region, and calculate a variance at the mean position in order to obtain variance. We apply the process to all of vaild horizontal positions in the search region, and then search for the mean position with the minimum variance. If the mean position is placed inner than the outter segment of the planar region, the boundary position is constrained to the outter segment position. The uncertainty of of the boundary position is obtained simultaneously. This process is applied to the stereo pair images. With the results, we can obatined the boundary position and its uncertainy using the stereo geometry.

By combining the obtained boundary position with the fitted plane by the method of section 3.1, the constrained boundary position $\boldsymbol{P}_b$ and its uncertainty $\boldsymbol{\Sigma}_{P_b}$ is estimated.

3.3 Modeling feature position

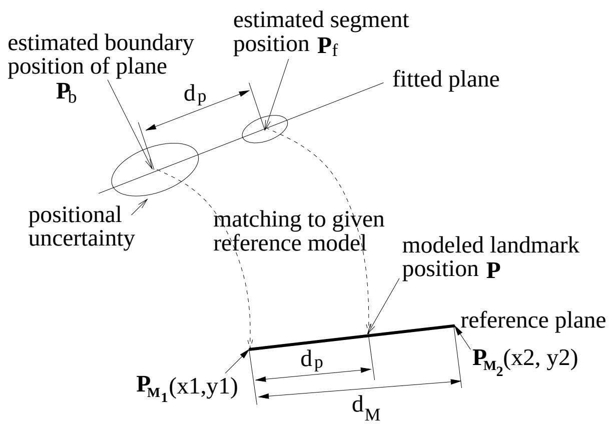

Figure 4: Modeling relative feature position with respect to the boundary position of the reference plane.

Given a reference plane with two edges $\boldsymbol{P}_{M_1} = [x_1\ y_1]^T$ and $\boldsymbol{P}_{M_2} = [x_2\ y_2]^T$, a feature position $\boldsymbol{P} = [x\ y]^T$ on the plane with relative distance d_p with respect to the boundary position $\boldsymbol{P}_{M_1}$ is obtained as follows:

$$\boldsymbol{P} = \begin{bmatrix} x_1 \\ y_1 \end{bmatrix} + \begin{bmatrix} \frac{d_p}{d_M}(x_2 - x_1) \\ \frac{d_p}{d_M}(y_2 - y_1) \end{bmatrix} \tag{15}$$

where d_M denotes length of the given reference plane (see Fig. 4), and d_p denotes a relative distance between the estimated boundary position $\boldsymbol{P}_b$ and a feature position $\boldsymbol{P}_f$.

Eq. (15) can be rewritten into the following non-linear equation form:

$$\boldsymbol{P} = \boldsymbol{M}(\boldsymbol{P}_{M_1}, \boldsymbol{P}_{M_2}, \boldsymbol{P}_b, \boldsymbol{P}_f) \tag{16}$$

Since the reference plane is already known, the positional uncertainty is zero. Then, the positional uncertainty of the feature, $\boldsymbol{\Sigma}_P$, is obtained as follows:

$$\boldsymbol{\Sigma}_P = \frac{\partial \boldsymbol{M}}{\partial \boldsymbol{P}_b} \boldsymbol{\Sigma}_{P_b} \frac{\partial \boldsymbol{M}}{\partial \boldsymbol{P}_b}^T + \frac{\partial \boldsymbol{M}}{\partial \boldsymbol{P}_f} \boldsymbol{\Sigma}_{P_f} \frac{\partial \boldsymbol{M}}{\partial \boldsymbol{P}_f}^T \tag{17}$$

where $\boldsymbol{\Sigma}_{P_b}$ and $\boldsymbol{\Sigma}_{P_f}$ denote the estimated uncertainties of the boundary and feature position by using EKF.

From Eq. (17), we can see that $\boldsymbol{\Sigma}_P$ is composed of uncertainties of the boundary and the feature position. As the rank of Eq. (17) is 1, the position and its uncertainty are constrained on the reference plane.

4 Stable landmark selection

To select stable landmarks from the modeled features, we utilize the segment position and the length similarity as selection criterions.

Since features on plane boundary are unstable, we fisrt filter out a near segment from the boundary position. We define the unstable boundary region as 3σ area and search for the stable landmarks whose the mean positions do not belong to the unstable region. Next, assuming that the low similarity of length between the pair of segments is unstable because the feature can be easily changed by viewpoints, the length similarity can be utilize as the selection criterion. The length similarity ℓ_s is expressed as follows:

$$\ell_s = \frac{min\{len(l), len(r)\}}{max\{len(l), len(r)\}} \tag{18}$$

where $len(i)$ denotes length of i segment. We filter out a feature pair with less similarity than a threshold. When the robot moves, it uses a subset of stable landmarks with less uncertainty for localization.

5 State estimate using Extended Kalman Filter

As the robot repeatedly observes the same landmark, positional uncertainty of the landmark can be estimated by using Kalman filter.

To estimate the robot and landmark state we set the robot and landmark state to the system state $\boldsymbol{S}$. Since the robot state is changed by a control input $\boldsymbol{U}_t$, the system equation is expressed by a non-linear form[3].

$$\boldsymbol{S}_{t+1} = \boldsymbol{F}(\boldsymbol{S}_t, \boldsymbol{U}_t) \tag{19}$$

Figure 5: Matched segments by using the segment-based stereo matching.

The constraint equation for the observation is expressed as follows:

$$G(S_t, L_t) = \mathbf{o} \tag{20}$$

In the same manner as section 3.1, the robot can estimate its own state and the landmark state simultaneously using EKF.

6 Experimental results

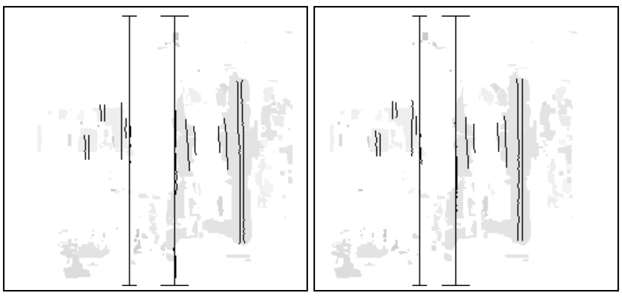

Figure 6: Matching results by the SAD-based stereo matching and fitted boundary edges: Gray regions are matched positions, and black vertical segments are selected matched segments. The long vertical lines are fitted boundary positions, and the positional uncertainties are shown by horizontal lines on the top and the bottom of the position.

We conducted an experiment in our lab scene shown in Fig. 5. The partition at the right side and the white board at the left side are located at the distance of 4[m] and 6[m] from the robot, respectively. The boundary position of the partition and the white board are $(0, 4000)$[mm] and $(-550, 6000)$[mm], respectively.

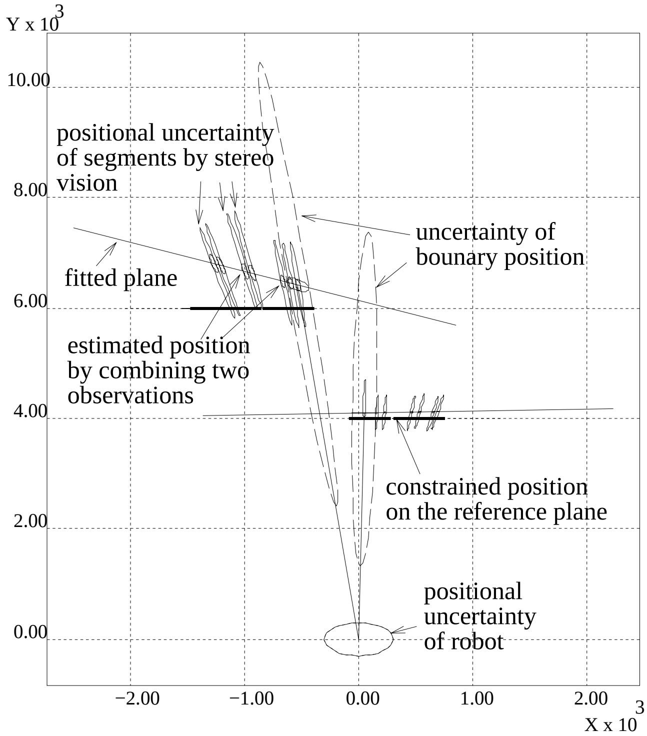

Figure 7: Positional uncertainty of the selected features.

First, the segment-based stereo matching is performed. In Fig. 5, several false matching are shown under white board.

Next, the SAD-based stereo matching with 15×15 window is applied to searching for good matched segments and the reference plane. Fig. 6 shows a result of the SAD matching.

At the current viewpoint, the robot can observe the partition and the white board as the reference plane. To select stable features, the robot extracts the planar region corresponding to the reference planes. From the extracted region, a set of segments in the corresponding plane is selected. To utilize the selected line segments as landmarks, the positional uncertainty of the segments is estimated from the constraint that each segment is on the reference plane.

Fig. 7 shows the positional uncertainty of the selected features. By combining the semgent position and the fitted plane using EKF, the positional uncertainty can be reduced.

Table 1 shows the estimated position and standard

Figure 8: Matched segments by only using segment-based stereo matching: the robot observes five landmarks in the partition plane.

Figure 9: Matched segments: the robot observes two landmarks in the partition plane.

deviation of the on-line selected landmarks. Unstable features such as feature 1 and 2 in the partition plane and feature 1, 2 and 3 in the white board plane are not selected a landmark. Since the partition is nearer, the landmarks on the plane have less positional uncertainty than the ones on the white board. We can also see that the positional uncertainty σ_y is zero because the landmarks are constrained on the reference plane.

With the modeled landmarks, the robot moves while observing landmarks for localizaition. Figs. 8 and 9 are input images when the robot moves 1[m] and 2[m] on the target trajectory which is planned using the given 2D obstacle map[3]. The robot contols its viewing direction to the midpoint of the boundary edges of the partition and the white board. In these two observation, the robot could observe all of the selected landmarks which are in the viewing area. This resuls show that the method actually selects stable landmarks.

Fig. 10 shows the motion results. As the result,

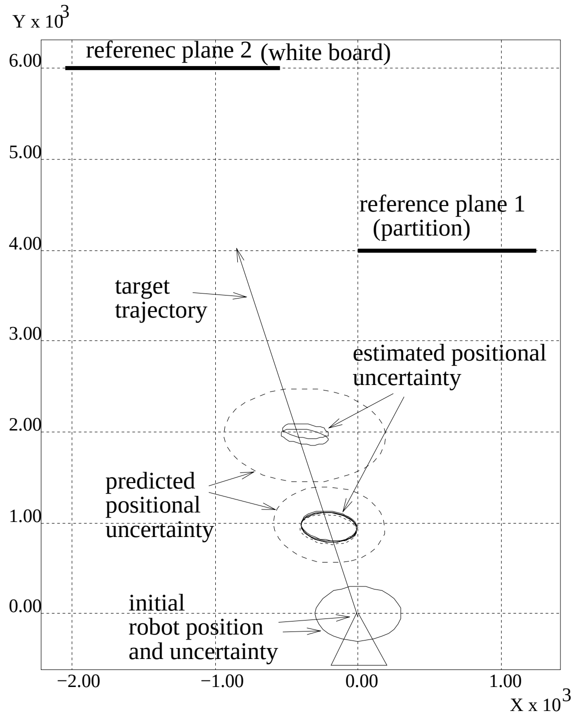

Figure 10: Motion result using on-line selected landmarks.

we can see that the uncertainty of the robot position can be reduced by observing the on-line modeled landmarks with positional uncertainty, so it is possible to execute motion without any knowledge about landmarks in advance. From the experemental resutls, we can see the proposed method is valid.

7 Conclusions and discussion

In this paper, we have proposed a method of selecting stable visual landmarks considering both their detectability from various viewpoints and the uncertainty of vision and motion. Since we select vertical line segments on a vertical plane as landmarks, the plane information in a given 2-D map is utilized to reduce the positional uncertainty of the selected landmarks. The experimental results in real scenes show the validity of the proposed method.

A future work is to integrate the proposed method with our previously developed viewpoint selection method[3] so that the robot can move safely and efficiently without being given landmarks in advance.

Table 1: Modeled features on the partition and the white board. [mm]

plane	index	x	y	l	σ_x	σ_y	ℓ_s	selected as landmark	reason
partition	1	0.1	4000.0	1309.0	28.3	0.0	0.5	No	near boundary
partition	2	109.4	4000.0	487.0	35.0	0.0	1.0	No	near boundary
partition	3	177.8	4000.0	270.0	35.0	0.0	0.9	Yes	
partition	4	411.0	4000.0	258.0	35.0	0.0	1.0	Yes	
partition	5	483.0	4000.0	490.0	35.0	0.0	1.0	Yes	
partition	6	605.1	4000.0	1542.0	35.0	0.0	1.0	Yes	
partition	7	643.7	4000.0	1557.0	35.8	0.0	1.0	Yes	
white board	1	-550.2	6000.0	584.0	54.2	0.0	0.8	No	near boundary
white board	2	-622.6	6000.0	279.0	46.4	0.0	0.9	No	near boundary
white board	3	-698.3	6000.0	841.0	47.0	0.0	1.0	No	near boundary
white board	4	-1004.3	6000.0	245.0	50.4	0.0	0.9	Yes	
white board	5	-1076.0	6000.0	261.0	51.0	0.0	0.9	Yes	
white board	6	-1309.9	6000.0	361.0	53.1	0.0	1.0	Yes	
white board	7	-1380.9	6000.0	376.0	53.9	0.0	1.0	Yes	

References

[1] C. Becker, J. Salas, K. Tokusei, and J. C. Latombe, "Reliable Navigation Using Landmarks," *Proc. of IEEE Int. Conf. on Robotics and Automation*, pp. 401-406, 1995.

[2] M. Betke and L. Gurvits, "Mobile Robot Localization Using Landmarks," *IEEE Trans. on Robotics and Automation*, Vol. 13, No. 2, pp. 251-263, 1997.

[3] I. Moon, J. Miura, and Y. Shirai, "Dynamic Motion Planning for Efficient Visual Navigation under Uncertainty," *Proc. 5th Int. Conf. on Intelligent Autonomous Systems*, pp. 172-179, 1998.

[4] R. Greiner and R. Isukapalli "Learning to Select Useful Landmarks," *IEEE Trans. on Systems, Man, and Cybernetics-PartB:Cybernetics* , Vol. 26, No. 3, pp. 437-449, 1996.

[5] S. Maeyama, A. Ohya, and S. Yuta, "Outdoor landmark map generation through human assisted route teaching for mobile robot navigation," *Proc. of IEEE/RSJ Int. Conf. on Intelligent Robots and Systems*, pp. 957-962, 1996.

[6] T. Kanbara, J. Miura, and Y. Shirai, "Selection of Efficient Landmarks for an Autonomous Vehicle," *Proc. of IEEE/RSJ Int. Conf. on Intelligent Robots and Systems*, pp. 1332-1338, 1993.

[7] J. Horn and G. Schmidt, "Continuous Localization for Long-Range Indoor Navigation of Mobile Robots," *Proc. of IEEE Int. Conf. on Robotics and Automation*, pp. 387-394, 1995.

[8] R. Talluri and J. K. Aggarwal, "Mobile Robot Self-Location Using Model-Image Feature Correspondence," *IEEE Trans. on Robotics and Automation*, vol. 12, No. 1, pp. 63-77, 1996.

[9] A. Arsenio and M. I. Ribeiro, "Active Range Sensing for Mobile Robot Localization," *Proc. of IEEE/RSJ Int. Conf. on Intelligent Robots and Systems*, pp. 1066-1071, 1998.

[10] J. J. Little, J. Lu, and D. R. Murray, Selecting Stable Image Features for Robot Localization Using Stereo, *Proc. of IEEE/RSJ Int. Conf. on Intelligent Robots and Systems*, pp. 1072-1077, 1998.

[11] J. Miura and Y. Shirai, "Vision and Motion Planning for a Mobile Robot under Uncertainty," *The Int. Journal of Robotics Research*, Vol. 16, No. 6, pp. 806-825, 1997.

[12] P. S. Maybeck, "The Kalman Filter:An Introduction to Concepts," in: I.J. Cox and G.T. Wilfong, eds., *Autonomous Robot Vehicles*, Springer-Verlag, pp. 194-204, 1990.

[13] S.H. Lee and J.J. Leou, "A Dynamic Programming Approach to Line Segment Matching in Stereo Vision," *Pattern Recognition*, Vol. 28, No. 8, pp. 961-986, 1994.